Decreased Expression of T-Cell-Associated Immune Markers Predicts Poor Prognosis in Patients with Advanced Follicular Lymphoma Received Rituximab Plus Bendamustine

Shinya Rai (rai@med.kindai.ac.jp)
Kindai University Faculty of Medicine Graduate School of Medical Sciences: Kinki Daigaku Igakubu Daigakuin Igaku Kenkyuka https://orcid.org/0000-0003-3929-9751

Hiroaki Inoue
Kindai University Hospital: Kinki Daigaku Byoin

Kazuko Sakai
Kindai University Hospital: Kinki Daigaku Byoin

Hitoshi Hanamoto
Kindai Nara Byoin: Kinki Daigaku Igakubu Nara Byoin

Mitsuhiro Matsuda
PL General Hospital

Yasuhiro Maeda
Minami Sakai Hospital

Takahiro Haeno
Kindai University Hospital: Kinki Daigaku Byoin

Yosaku Watatani
Kindai University Hospital: Kinki Daigaku Byoin

Takahiro Kumode
Kindai University Hospital: Kinki Daigaku Byoin

Kentarou Serizawa
Kindai University Hospital: Kinki Daigaku Byoin

Yasuhiro Taniguchi
Kindai University Hospital: Kinki Daigaku Byoin

Chikara Hirase
Kindai University Hospital: Kinki Daigaku Byoin

J. Luis Espinoza
Kindai University Hospital: Kinki Daigaku Byoin

Yasuyoshi Morita
Kindai University Hospital: Kinki Daigaku Byoin

Hirokazu Tanaka

Kindai University Hospital: Kinki Daigaku Byoin
Takashi Ashida
Kindai University Hospital: Kinki Daigaku Byoin
Yoichi Tatsumi
Kindai University Hospital: Kinki Daigaku Byoin
Kazuto Nishio
Kindai University Hospital: Kinki Daigaku Byoin
Itaru Matsumura
Kindai University Hospital: Kinki Daigaku Byoin

Research

Keywords: Follicular lymphoma, Bendamustine, Lymphopenia, T-cell, Tumor microenvironment, POD24

Posted Date: July 8th, 2021

DOI: https://doi.org/10.21203/rs.3.rs-648976/v1

Abstract

Background: Several clinical risk stratification models have been proposed to predict the clinical outcomes of follicular lymphoma (FL) cases, however, few reports are available to predict prognosis of FL cases receiving bendamustine-based regimens. We previously examined the utility of rituximab-bendamustine (RB) treatment for newly diagnosed advanced FL, who showed non-optimal responses to two cycles of R-CHOP therapy.

Methods: In this study, we explored the biomarkers that could influence outcomes for the RB-treated FL cases in the context of the prospective cohort by target capture and sanger sequencing, and gene-expression profiling analyses using 50 diagnostic biopsies.

Results: We first examined the mutational status of 410 genes in tumor specimens derived from RB-treated cases. As reported before, *CREBBP*, *KMT2D*, *MEF2B*, *BCL2*, *EZH2*, *CARD11, TNFRSF14, EP300,* and *APC* were recurrently mutated, however, none of which was predictive for progression-free survival (PFS) in RB-treated cases. Similarly, the m7-FLIPI did not correlate with PFS or progression of disease within 24 months (POD24). A gene expression analysis using a panel of 770 genes associated with carcinogenesis and/or immune response showed that the expression of CD8+ T-cell markers (*GZMM, FLT3LG, CD8A, CD8B, GZMK*) and half of the genes regulating Th1 and Th2 responses were significantly lower in the POD24 group than in the noPOD24 group. Finally, we selected 10 genes (*TBX21, CXCR3, CCR4, CD8A, CD8B, GZMM, FLT3LG, CD3E, EOMES, GZMK*), and dichotomized RB-treated cases into immune infiltration^{high} (infil^{high}) and infiltration^{low} (infil^{low}) clusters. The 3-years PFS rate was lower in the infil^{low} cluster than in the infil^{high} cluster (50.0% [95% CI: 27.1–69.2%] *vs*. 84.2% [95% CI: 58.7–94.6%], p=0.0237). Of note, the proportion of cases with peripheral lymphopenia (<869/mL) at diagnosis was higher in the infil^{low} cluster than in the infil^{high} cluster (38.5% *vs*. 9.09%, OR: 6.25 [95%CI, 1.20-32.7], p=0.0235).

Conclusion: These results suggest that the T-cell-associated immune markers could be useful to predict prognosis in RB-treated FL cases.

Trial registration: This trial was retrospectively registered in UMIN on April. 24, 2014 (UMIN000013795; http://www.umin.ac.jp/icdr/index-j.html).

Background

Follicular lymphoma (FL) is the most common indolent subtype of B-cell non-Hodgkin lymphomas[1]. The majority of FL patients present with advanced stages[1], and those with high tumor burden and/or disease-related symptoms require immunochemotherapy.

To date, several chemotherapy regimens, including CHOP (cyclophosphamide, doxorubicin, vincristine, and prednisone), CVP (cyclophosphamide, vincristine, and prednisone), and bendamustine (B) in combination with anti-CD20 monoclonal antibodies such as rituximab (R) or obinutuzumab (G)[2,3] have

been recommended as front-line therapies in several guidelines[4–8]. Most of the FL patients receiving these front-line immunochemotherapy regimens can obtain long-term survival benefit[9]. However, about 10–20% of the patients experience progression of disease within 24 months of diagnosis or treatment initiation (which is called POD24), and these patients have a substantially increased risk of death within 5 years after diagnosis[9–12].

Given the heterogeneity of disease courses, several clinical risk stratification models, including Follicular lymphoma International Prognostic Index (FLIPI-1 and FLIPI-2), PRIMA-PI, and FLEX were proposed to predict the clinical outcomes of FL patients such as progression-free survival (PFS) and overall survival (OS)[13–16]. However, all of these models have limited value to predict POD24. Meanwhile, accumulated findings from genetic and gene-expression profiling analyses showed that several molecular risk models mainly based on the intrinsic tumor properties, such as m7-FLIPI[17], POD24-PI[18] and 23-gene-expression profiling (GEP) score[19,20], were shown to be a useful tool to identify FL patients at high- or low-risk of progression after treatment with immunochemotherapy. In addition, a gene expression signature based on the extrinsic tumor environment, particularly focusing on the tumor microenvironment (TME) of FL, was established to predict POD24[11]. However, these models are mainly based on the data from the patients who received R-CHOP or R-CVP, and few reports are available to predict the prognosis of FL patients receiving B-based regimens.

We previously conducted a multicenter prospective phase 2 (CONVERT) trial, and demonstrated the utility of RB for treatment-naive advanced FL showing non-optimal responses (nOR) to the initial two cycles of R-CHOP therapy[21]. In addition, we reported that peripheral lymphopenia (< 869/uL) before treatment was an independent poor prognostic factor for RB-treated FL patients in both our trial and validation cohorts[21]. Thus, the main object of this study is to identify molecular biomarker(s) that could predict outcomes of RB-treated FL patients by genetic and gene-expression profiling analyses.

Methods

Study design and patients

The design and characteristics of the registered patients in the CONVERT trial were described previously[21]. In brief, newly diagnosed adult patients with advanced (stage III/ IV or stage II with bulky disease), CD20-positive FL, with histologic grade 1-3a (excepting low FLIPI-2) were eligible for this trial. All patients initially received two cycles of standard R-CHOP. Patients who achieved complete response (CR) /complete response unconfirmed (CRu) according to Cheson's morphological criteria 1999[22] (defined as an optimal response [OR] group) further received 4-6 cycles of R-CHOP treatment. The remaining patients who failed to achieve CR/CRu (defined as a non-optimal response [nOR] group), subsequently received six cycles of RB (R 375 mg/m^2 d1, B 90 mg/m^2 d1-2) every 28 days.

This study was designed and conducted according to the Declaration of Helsinki and was registered in UMIN (000013795) and jRCT (051180181). All patients provided written informed consent.

The protocol, informed consent forms, and any amendments were approved by the institutional review boards of each hospital and certified review board.

Target capture sequencing assay

DNA was extracted from formalin-fixed paraffin-embedded (FFPE) samples using a DNA storm kit (Cell Data Sciences, Inc). The targeted DNA library for panel sequencing that comprises approximately 1.65 Mb coding regions of all exons in 409 genes (**Supplementary Table 1**) was constructed using an Oncomine Tumor Mutation Load Assay (Thermo Fisher Scientific) according to the manufacturer's protocol. In brief, 20 ng DNA was subjected to multiplex PCR amplification with an Ion AmpliSeq Library Kit 2.0. After multiplex PCR, Ion Xpress Barcode Adapters (Thermo Fisher Scientific) were ligated to the PCR products, which were then purified with the use of AMPure XP beads (Beckman Coulter, Brea, CA). The purified libraries were pooled and then sequenced with an Ion Torrent S5 instrument and Ion 550 Chip Kit (Thermo Fisher Scientific). DNA sequencing data were accessed through the Torrent Suite ver. 5.10 program (Thermo Fisher Scientific). Reads were aligned against the hg19 human reference genome, and variants were analyzed with the use of Ion reporter ver. 5.10 (Thermo Fisher Scientific). Raw variant calls were manually checked using the integrative genomics viewer (IGV, Broad Institute). In this analysis, we defined the following criteria for the sequence quality (1) the uniformity of amplicon coverage of >60%, (2) the minimum quality criterion was 80% of target bases with ≥ 100x sequencing coverage. The mutations were filtered with the exclusion of (1) Fisher's exact P-value <0.01, (2) Phred QUAL score of <99, (3) allele frequency in tumor <0.025, and missense SNVs with an allele frequency of 0.45–0.55 in copy-neutral regions, unless they were listed in the COSMIC database (v70) or reported to be mutated in FL. Germline mutations were excluded with the NCBI dbSNP build 131 and UCSC genome browser database[23,24].

Sanger sequencing analysis

Exon 2 and 3 of *MEF2B* were analyzed using the PCR primers designed with Primer3 (**Supplementary Table 2**). The *MEF2B* coding exons 2 and 3 were amplified by PCR as described previously[25]. After denaturation step at 94°C for 5 min, PCR consisting of denaturation (94°C for 30 sec) annealing (56°C for 30 sec), and extension steps (72°C for 30 sec) were repeated until 35 cycles, followed by final extension step at 72°C for 7 min on a GeneAmp PCR system 9700 (Thermo Fisher Scientific). After visual confirmation of amplification, the PCR product was submitted for sanger sequence analysis as previously described[25].

The m7-FLIPI score calculation

The m7-FLIPI score was calculated by using the calculator presented at the German Low-Grade Lymphoma Study Group official internet site (www.glsg.de/m7-flipi/). The same cut-off level as used in the original publication was applied to determine high- and low-risk categories (m7-FLIPI score ≥0.8 and <0.8, respectively)[17].

Gene-expression profiling analysis

RNA was extracted from FFPE samples using an RNA storm kit (Cell Data Sciences, Inc). Details of the nCounter assay (NanoString Technologies, Seattle, WA, USA) have been reported previously[24,26]. In this study, the customized PanCancer immune-profiling panel (NanoString Technologies), which consists of 770 genes related to cancer or immune cells and additional 30 genes (**Supplementary Table 3**), was used for nCounter-based gene-expression measurements. The data were analyzed by using nSolver 4.0 software (NanoString) and JMP version 13.0 software (SAS Institute).

Statistical analysis

The cutoff date for this analysis was December 31, 2019. The survival analysis was performed by the Kaplan-Meier method, which was evaluated by a log-rank test. Fisher's exact test was used for between-categorical data comparisons. For the comparison of two continuous variables data were tested by Wilcoxon rank sum test. Statistical analyses were performed with R 4.1.0 software (The R Foundation for Statistical Computing), and p value <0.05 was considered statistically significant.

Results

Patient characteristics and clinical outcomes

A total of fifty-six patients initially received two cycles of R-CHOP. Then, 13 patients (23.2%), who achieved CR/CRu (optimal response [OR]-group), continued R-CHOP for further 4-6 cycles. The remaining 43 patients (76.8%), who were judged as nOR, received RB as the protocol treatment. The FFPE samples were available for extracting sufficient and undegraded DNA and/or RNA in 50/56 cases (89.3%) for this study. The baseline characteristics of these 50 cases were shown in **Table 1**. At a median follow-up time of 47.4 months (range: 3.20–79.3), PFS and OS rates at 3 years in all cases (n=50) were 71.0% (95% CI: 56.0-81.7%) and 93.5% (95% CI: 81.2-97.9%), respectively (**Supplementary Fig. 1a, b**). The 3-years PFS rates were 87.5% in the OR-group (95% CI: 38.7-98.1%) and 67.5% in the nOR-group (95% CI: 50.7-9.7%), respectively, with no statistically significant difference (p=0.213). The 3-years OS rates were 100% in the OR-group (95% CI: not applicable) and 92.2% in the nOR-group (95% CI: 77.6-97.4%, p=0.283) (**Supplementary Fig. 1c,1d**).

Mutational landscape of the whole population

To investigate the mutational landscape in this cohort, we performed the target capture sequence using tumor samples from the above described 50 cases. Eight cases were excluded from this analysis because of their poor DNA qualities. Thus, 42 cases (OR n=8; nOR n=34) were analyzed on the targeted panel for 409 genes, in which most of the recurrently mutated genes in FL were included excepting *MEF2B*. *MEF2B* encodes a transcriptional activator and is mutated in 10～20% of FL and its mutational status is applied in m7-FLIPI[27]. Thus, we analyzed its mutation status by sanger sequencing independently. In this analysis, we focused on the exon 2 and exon3 of *MEF2B*, because most of *MEF2B*

mutations in FL were scattered around these regions[28]. As a result, *MEF2B* mutations were identified in 13/42 cases (31.0%), all consisting of *L67R* in the exon 3, which mutated site was reported to play an important role in the interaction with EP300 proteins[28]. The double mutations with *L67R* and *G2R* in exon 2 were identified in one case (**Fig. 1a**).

When the results from target capture sequencing and sanger sequencing were combined, a total of 34 genes was found to be recurrently mutated (in ≥2 cases), including 107 non-synonymous single nucleotide variants (SNVs), 19 multiple mutations, 16 frameshift insertions or deletions, 13 stop-gain mutations, and 7 non-frameshift insertions or deletions. Overall, 37/42 cases (88.1%) had at least one coding mutation within 410 genes with a median of 4 mutations per patient (range 0–10) (**Fig. 1a**), and the average depth of sequencing coverage in the 37 cases was 882X (103-3,999X). The most recurrently mutated genes were *CREBBP* (59.5%), *KMT2D* (38.1%), *MEF2B* (31.0%), *BCL2* (28.6%), *EZH2* (21.4%), *CARD11* (16.7%), *TNFRSF14*, and *EP300* (14.3% each), *APC* (11.9%), with the landscape closely resembling the previous reports[1,29,30] (**Fig. 1b**). Positions and types of somatic mutations in these genes were shown in **Supplementary Fig. 2**.

Association of mutation profile with clinical outcomes in the nOR-group

Among recurrently mutated genes, their mutation frequencies (in ≥10%) in the OR- and nOR-groups were shown in **Table 2**. Next, we analyzed whether mutation status influenced the outcomes in the nOR-group (n=34). As shown in **Fig. 2a**, the mutation status of the specific gene did not influence PFS significantly in univariate analyses. We also evaluated the influence of gene mutations on POD24. Among 7 cases with POD24 and 27 cases without POD24, 28.6% (2/7) of POD24 cases harbored *PTEN* or *CIC* mutations as compared with 0% (0/27) in cases without POD24, with a statistical difference (p=0.0374) (**Fig. 2b**). Interestingly, no POD24 event occurred in RB-treated cases with *CARD11* mutations in the nOR-group. In addition, the cases with *CARD11* mutations tended to have better 3-years PFS rates than unmutated cases but with no statistically significant difference (100% vs. 59.3%, p=0.174) (**Fig. 2c**).

Association of m7-FLIPI with clinical outcomes

We next investigated whether m7-FLIPI could be applied to this total cohort (n=42). As expected, no cases (0/8) in the OR-group were classified into the high-risk category in the m7-FLIPI as compared with 29.4% (10/34) in the nOR-group but without a significant difference (p=0.165) (**Table 2**). The high-risk group tended to have an inferior 3-years PFS rate than the low-risk group (76.8% [95% CI: 57.4%–88.2%] *vs.* 60.0% [95% CI: 25.3%–82.7%]) but without a significant difference (p=0.104) (**Fig. 3a**).

Next, we focused on RB-treated cases (n=34) in the nOR-group. In this group, the proportion of cases in the low- and high-risk category in m7-FLIPI was 70.6% (24/34) and 29.4% (10/34), respectively (**Table 2**). At a median follow-up time of 48.7 months (4.07-79.3), the 3-years PFS rates were 70.8% in the low-risk group (95% CI: 48.4-84.9%) and 60.0% in the high-risk group (95% CI: 25.3-82.7%), respectively, without a significant difference (p=0.264) (**Fig. 3b**). Among 24 cases in the low-risk group, 4 cases

experienced POD24 (16.7%), while 3 from 10 cases in high-risk group experienced POD24 (30%) without a significant difference (OR: 0.467, [95%CI: 0.0830-2.62], *p*=0.394) (**Fig. 3c**).

Association of the 23-gene expressions with clinical outcomes

We next analyzed gene expression levels by nCounter system using the FFPE samples from 48 cases. Sample quality was assessed by mRNA levels of 40 housekeeping genes in each sample (**Supplementary Table 3**). It was previously reported that the GEP score based on the expression of 23 genes was associated with clinical outcomes of FL cases[19], which was confirmed by the following study[20]. Furthermore, the 23 genes could identify two main clusters characterized by high- or low-expression associated with favorable and poor outcomes[20]. So, we subjected our 48 cases to hierarchical clustering using these 23 genes. Consistent with the previous reports[19,20], we could identify two main clusters (cluster 1 and cluster 2) (**Fig. 4a**), however, at a median follow-up time of 47.4 months (3.2-79.3), 3-years PFS rates did not differ significantly between the two clusters (74.7% [95% CI: 55.6%–86.5%] *vs.* 60.0% [95% CI: 31.8%–79.7%], *p*=0.436) (**Fig. 4b**).

Next, we compared 3-years PFS between the cluster 1 and 2 in the RB-treated 39 cases. At a median follow-up time of 46.1 months (3.2-79.3), the cases in cluster 2 tended to have an inferior 3-years PFS rate compared with those in cluster 1 (50.0% [95% CI: 18.4%–75.3%] *vs.* 72.4% [95% CI: 52.3%–85.1%]) but without a significant difference (*p*=0.263) (**Fig. 4c**). We further compared the expression of 23 genes between 8 cases with POD24 and 31 cases without POD24. Although these genes were reported to portend good or poor risk, the expression levels of these genes were almost equivalent in the two groups (**Supplementary Fig. 3**).

Association of the T-cell-associated gene expressions with clinical outcomes

In this trial, we previously reported that a low absolute lymphocyte count (ALC) was an independent poor prognostic factor for RB-treated patients[21]. Because lymphopenia was considered to reflect an immune-suppressive state, we applied the customized pan-cancer immune-profiling panel, which consists of 770 genes related to cancer development and/or immune reactions, to the RB-treated cases in the nOR-group (n=39). As a result, a total of 33 genes, including 2 upregulated (*CD79a* and *POU2F2*) and 31 downregulated genes (each with log2 fold change > |0.5|, and corrected [-log10*P*] >1.5) were differentially expressed in the POD24 group (n=8) compared with in the noPOD24 group (n=31). Of interest, the top genes downregulated in the POD24 group were markedly enriched with the T-cell-associated genes (**Fig. 5a**).

Thus, we further compared the expression levels of molecules specific for various types of T cells (Th1, Th2, and Th17, T follicular helper [Tfh], regulatory T [Treg], NK, and $CD8^+$ T cells) and of immune checkpoint markers between the two groups. Interestingly, the expression of $CD8^+$ T cell markers (*GZMM, FLT3LG, CD8A, CD8B, GZMK*) except for *PRF1* was significantly lower in the POD24 group than in the noPOD24 group (**Fig. 5b**). Furthermore, about half of the genes related to Th1 and Th2 responses in T

cells were downregulated in the POD24 group compared to those in the noPOD24 group. In contrast, Treg, NK, and immune checkpoint markers were almost equivalently expressed in the two groups (**Supplementary Fig. 4**).

Next, we selected 10 genes (*TBX21, CXCR3, CCR4, CD8A, CD8B, GZMM, FLT3LG, CD3E, EOMES, GZMK*) by manual curation to integrate biological aspects mainly focused on the $CD8^+$ T cell, and performed unsupervised hierarchical clustering using these genes. As a result, we could dichotomize 39 RB-treated cases into immune infiltration^{high} (infil^{high}) and infiltration^{low} (infil^{low}) clusters (**Fig. 5c**). The 3-years PFS rate was significantly lower in the infil^{low} cluster than in the infil^{high} cluster (50.0% [95% CI: 27.1%–69.2%] *vs*. 84.2% [95% CI: 58.7%–94.6%], p=0.0237) (**Fig. 5d**). Of note, POD24 was observed in 8/20 (40%) cases in the infil^{low} cluster, and no POD24 event occurred in the infil^{high} cluster with a significant difference (p=0.0084) (**Fig. 5e**).

Association of the T-cell-associated gene expressions with their mutation profile

We finally analyzed whether gene mutations influence the expression of T-cell-associated genes in all cases. However, the frequencies of mutations were roughly the same between infil^{low} and infil^{high} clusters in most genes (**Fig. 6a**). For example, the mutation frequencies in *CREBBP*[31], *EZH2*[32], and *T/NFSF14*[33], which are supposed to regulate the tumor microenvironment, did not differ significantly between the two clusters. In contrast, a significant difference was noticed for the *CARD11* mutations. In the infil^{high} cluster, 31.2% (6/19) of the cases harbored *CARD11* mutations compared to 4.76% (1/21) in the infil^{low} cluster (p=0.0395) (**Fig. 6b**). Of note, the proportion of cases with low ALCs was higher in the infil^{low} cluster than in the infil^{high} cluster (38.5% *vs*. 9.09%, OR: 6.25 [95%CI, 1.20-32.7], p=0.0235) (**Fig. 6c**).

Discussion

In this study, we attempted to identify biomarker(s) that can predict clinical outcomes of RB-treated FL cases. At first, we examined gene mutational profiles in our cases. As a result, we found that types of mutated genes and their frequencies were roughly the same as previously reported[1,29,30], and we found that none of those mutations influenced PFS in univariate analyses. Among them, mutations of *CARD11*, which functions as a positive regulator of the NF-kB pathway in normal B and T lymphocytes, were detected in 16.7% of the cases (7/42). *CARD11* mutation is more frequently observed in transformed FL than in untransformed FL[29,34] and counted as a poor prognostic factor in m7-FLIPI[17]. In accord with these results, all cases harboring *CARD11* mutations didn't show optimal responses to the initial 2 cycles of R-CHOP and were classified into the nOR-group. However, all these cases achieved and maintained CR at least for 3 years by the early conversion to RB treatment. These results raised a possibility that the negative impact of *CARD11* mutations observed under R-CHOP treatment might be canceled by RB treatment. Meanwhile, 28.6% (2/7) of RB-treated cases with POD24 harbored *PTEN* or *CIC* mutations as compared with 0% (0/27) in cases without POD24 with a statistical difference (p = 0.0374). However,

further studies are necessary to elucidate the clinical significance of *PTEN* or *CIC* mutations in RB-treated FL cases.

We also assessed whether m7-FLIPI is useful to predict prognosis of our RB-treated FL cases. Although the 3-years PFS tended to be higher in the m7-FLIPI low group than in the m7-FLIPI high group (70.8% *vs*. 60.0%), this difference was not significant ($p = 0.264$). Also, whereas m7-FLIPI was reported to be able to predict POD24 in R-CHOP-treated FL patients, POD24 was observed regardless of m7-FLIPI risk groups in our BR-treated cases (high 30% *vs*. low 16.7%, $p = 0.394$). It must be noted that although the results reported in this study may lack statistical power due to the small number of cases. In accord with our results, however, m7-FLIPI had no prognostic value in RB- or GB (G + B)-treated FL cases, as reported in a randomized phase III (GALLIUM) trial[3,35]. Together, these results suggest that m7-FLIPI may not be an accurate prognostic factor in FL cases treated with B-based regimens.

The GEP score based on the expression of 23 genes was initially established to predict clinical outcomes in FL patients[19], and based on the 23-gene expression panel, it was possible to identify two main clusters associated with favorable and poor outcome in the subsequent study[20]. However, these studies included only a few cases treated with RB. Subsequently, this model was shown to have no prognostic value in RB- or GB-treated cohort in the GALLIUM study[36]. In accord with this result, we found that the 3-years PFS rates didn't differ between the cases in cluster 1 and cluster 2 (72.4% *vs*. 50.0%, $p = 0.263$). However, cluster 2 cases tended to have an inferior 3-years PFS rate compared with cluster 1 cases. Considering the small number of cases in this study, further studies are needed to draw a definite conclusion as to the efficacy of this model in predicting the prognosis of B -treated FL cases.

Several lines of evidence indicate that tumor cells depend on the interactions with non-malignant cells that constitute TME for their growth and survival[1,37]. Particularly, because of the indolent feature of FL cells, the prognosis of FL is substantially affected by TME, which consists of various types of T lymphocytes (cytotoxic T cells [CTLs], Tregs, and so on), B lymphocytes, and tumor-associated macrophages (TAMs). These cells act as positive or negative regulators of immune response in FL, thereby influencing the clinical outcomes in this disease. Based on this concept, Tobin JWD, *et al*. analyzed the immune infiltration profile in FL cases with or without POD24, and observed that a low expression of immune effectors (TNFα, CD4), checkpoints [programmed death-ligand 2 (PD-L2)], or macrophage markers (CD68), were associated with POD24. Among them, PD-L2 was the most sensitive marker in identifying patients with poor prognosis in R-CHOP-treated patients[11].

To elucidate the roles of the immune microenvironment in RB-treated FL cases, we have applied the customized pan-cancer immune-profiling panel consisting of 770 genes to the RB-treated cases in the nOR-group. As a result, we found that $CD8^+$ T cell markers such as *CD8A*, *CD8B*, *FLT3LG*, *GZMM*, and *GZMK*, were downregulated in the POD24 group, while markers for Treg and NK/T cells and immune checkpoint molecules were almost equivalently expressed in cases with or without POD24. Among the genes downregulated in the POD24 group, *GZMM* and *GZMK*, which are commonly expressed in CTLs and NK cells, have pro-apoptotic activities on tumor cells[38]. A low expression of *GZMM* and *GZMK* in

tumor tissues was associated with an unfavorable prognosis in cutaneous melanoma[39], and *GZMK* was also found to be downregulated in the process of FL transformation[40]. Together, these results suggest that anti-FL immune responses may be weakened in RB-treated FL cases undergoing POD24. However, future studies using high throughput technologies, such as single cell transcriptome sequencing, multicolor immunohistochemistry, and imaging mass cytometry are needed to determine which T cell subpopulations indeed express each cytotoxic molecule.

We further classified RB-treated cases into infil^{high} and infil^{low} clusters using manually selected 10 genes (*TBX21, CXCR3, CCR4, CD8A, CD8B, GZMM, FLT3LG, CD3E, EOMES, GZMK*). The PFS rate at 3 years was significantly lower in the infil^{low} cluster than in the infil^{high} cluster ($p = 0.0237$). In addition, POD24 was observed in 8/20 (40%) cases in the infil^{low} cluster, while none of infil^{high} cases underwent POD24 ($p = 0.0084$). These results suggest that our classification would be useful to predict clinical outcomes including POD24 in RB-treated FL cases. Also, given the results presented here, the combination of RB with a novel therapy, which can restore the number and/or function of T cells such as lenalidomide[41,42], would be a promising strategy to improve prognosis of the cases with infil^{low} immune profile. However, it should be noted that our RB-treated cases constitute a unique population, namely those who received RB after two cycles of R-CHOP. Therefore, future studies are required to determine whether our results are applicable to *de novo* FL cases treated with a B-based regimen as the 1st -line treatment using larger prospective cohorts.

To clarify molecular mechanisms underlying the difference in infil^{low} and infil^{high} immune profiles, we compared the frequency of mutations in both clusters. However, the frequencies of mutations were roughly the same between infil^{low} and infil^{high} clusters in most genes, especially that regulate TME such as *CREBBP, EZH2*, and *T/NFSF14*, excepting *CARD11*. These results raise the possibility that epigenetic regulation might be different between the two clusters. Of importance, the only significant clinical parameter related to the infil^{low} immune profile was lymphopenia, which we previously identified as a poor prognostic marker for RB-treated cases [21]. These results suggest that lymphopenia at diagnosis may reflect reduced T cell-mediated immune reactions in the TME and that it may be able to substitute for the immune profiling utilized in this study.

Conclusions

We here found that the expression of CD8$^+$ T cell markers was significantly lower in RB-treated cases with POD24 than those without POD24. Furthermore, FL cases were classified into infil^{low} and infil^{high} clusters based on the expression of T cell-associated genes, which was useful to predict the prognosis of RB-treated FL cases.

Abbreviations

RB: rituximab-bendamustine

FL: follicular lymphoma

B: bendamustine

R: rituximab

G: obinutuzumab

POD24: progression of disease within 24 months

FLIPI: Follicular lymphoma International Prognostic Index

PFS: progression-free survival

OS: overall survival

TME: tumor microenvironment

CR: complete response

Cru: complete response unconfirmed

FFPE: formalin-fixed paraffin-embedded

SNVs: single nucleotide variants

GEP: gene-expression profiling

ALC: absolute lymphocyte count

Tfh: T follicular helper

Treg; regulatory T

infil^{high}: immune infiltration^{high}

infil^{low}: immune infiltration^{low}

CTLs: cytotoxic T cells

TAMs: tumor-associated macrophages

FDCs: follicular dendritic cells

GELF: Groupe d'Etude des Lymphomes Folliculaires

Declarations

Ethics approval and consent to participate

This study was designed and conducted according to the Declaration of Helsinki and was registered in UMIN (000013795) and jRCT (051180181). All patients provided written informed consent. The protocol, informed consent forms, and any amendments were approved by the institutional review boards of each hospital and certified review board.

Consent for publication

Not applicable

Availability of data and materials

The datasets generated and/or analyzed during the current study are available in the source data files. (Persistent web link to datasets)

Competing interests

I.M. has received research funding from Chugai and Eizai Pharmaceuticals. S.R. has received payment for lectures from Chugai Pharmaceuticals.

No other potential conflicts of interest were reported.

Funding

Not applicable

Author contribution

S.R. and Y.T. designed and H.T., and I.M., supervised the research. S.R., H.I., H.H., M.M., Y.M., Y.W., C.H., T.H., T.K., K.S., Y.T., Y.M., T.A., K.S., K.N., and H.T. contributed to date collection and analysis. S.R., and H.T. performed statistical analysis. S.R., Y.W., K.S., K.N., H.T. and I.M. performed the research and prepared figures and tables. S.R., L.E. and H.T., and I.M. wrote the manuscript. And all authors read and approved the manuscript.

Acknowledgements

The authors thank the patients who participated in the study, their supporters, the investigators, and clinical research staff from the study centers.

References

1. Carbone A, Roulland S, Gloghini A, et al. Follicular lymphoma. Nat Rev Dis Primers. 2019;5(1):83.

2. Hiddemann W, Barbui AM, Canales MA, et al. Immunochemotherapy With Obinutuzumab or Rituximab for Previously Untreated Follicular Lymphoma in the GALLIUM Study: Influence of Chemotherapy on Efficacy and Safety. J Clin Oncol. 2018;36(23):2395-2404.

3. Marcus R, Seymour JF, Hiddemann W. Obinutuzumab Treatment of Follicular Lymphoma. N Engl J Med. 2017;377(26):2605-2606.

4. Federico M, Luminari S, Dondi A, et al. R-CVP versus R-CHOP versus R-FM for the initial treatment of patients with advanced-stage follicular lymphoma: results of the FOLL05 trial conducted by the Fondazione Italiana Linfomi. J Clin Oncol. 2013;31(12):1506-1513.

5. Luminari S, Ferrari A, Manni M, et al. Long-Term Results of the FOLL05 Trial Comparing R-CVP Versus R-CHOP Versus R-FM for the Initial Treatment of Patients With Advanced-Stage Symptomatic Follicular Lymphoma. J Clin Oncol. 2018;36(7):689-696.

6. Rummel MJ, Niederle N, Maschmeyer G, et al. Bendamustine plus rituximab versus CHOP plus rituximab as first-line treatment for patients with indolent and mantle-cell lymphomas: an open-label, multicentre, randomised, phase 3 non-inferiority trial. Lancet. 2013;381(9873):1203-1210.

7. Flinn IW, van der Jagt R, Kahl BS, et al. Randomized trial of bendamustine-rituximab or R-CHOP/R-CVP in first-line treatment of indolent NHL or MCL: the BRIGHT study. Blood. 2014;123(19):2944-2952.

8. Flinn IW, van der Jagt R, Kahl B, et al. First-Line Treatment of Patients With Indolent Non-Hodgkin Lymphoma or Mantle-Cell Lymphoma With Bendamustine Plus Rituximab Versus R-CHOP or R-CVP: Results of the BRIGHT 5-Year Follow-Up Study. J Clin Oncol. 2019;37(12):984-991.

9. Sarkozy C, Maurer MJ, Link BK, et al. Cause of Death in Follicular Lymphoma in the First Decade of the Rituximab Era: A Pooled Analysis of French and US Cohorts. J Clin Oncol. 2019;37(2):144-152.

10. Casulo C, Byrtek M, Dawson KL, et al. Early Relapse of Follicular Lymphoma After Rituximab Plus Cyclophosphamide, Doxorubicin, Vincristine, and Prednisone Defines Patients at High Risk for Death: An Analysis From the National LymphoCare Study. J Clin Oncol. 2015;33(23):2516-2522.

11. Tobin JWD, Keane C, Gunawardana J, et al. Progression of Disease Within 24 Months in Follicular Lymphoma Is Associated With Reduced Intratumoral Immune Infiltration. J Clin Oncol. 2019;37(34):3300-3309.

12. Seymour JF, Marcus R, Davies A, et al. Association of early disease progression and very poor survival in the GALLIUM study in follicular lymphoma: benefit of obinutuzumab in reducing the rate of early progression. Haematologica. 2019;104(6):1202-1208.

13. Solal-Céligny P, Roy P, Colombat P, et al. Follicular lymphoma international prognostic index. Blood. 2004;104(5):1258-1265.

14. Federico M, Bellei M, Marcheselli L, et al. Follicular lymphoma international prognostic index 2: a new prognostic index for follicular lymphoma developed by the international follicular lymphoma prognostic factor project. J Clin Oncol. 2009;27(27):4555-4562.

15. Bachy E, Maurer MJ, Habermann TM, et al. A simplified scoring system in de novo follicular lymphoma treated initially with immunochemotherapy. Blood. 2018;132(1):49-58.

16. Mir F, Mattiello F, Grigg A, et al. Follicular Lymphoma Evaluation Index (FLEX): A new clinical prognostic model that is superior to existing risk scores for predicting progression-free survival and early treatment failure after frontline immunochemotherapy. Am J Hematol. 2020;95(12):1503-1510.

17. Pastore A, Jurinovic V, Kridel R, et al. Integration of gene mutations in risk prognostication for patients receiving first-line immunochemotherapy for follicular lymphoma: a retrospective analysis of a prospective clinical trial and validation in a population-based registry. Lancet Oncol. 2015;16(9):1111-1122.

18. Jurinovic V, Kridel R, Staiger AM, et al. Clinicogenetic risk models predict early progression of follicular lymphoma after first-line immunochemotherapy. Blood. 2016;128(8):1112-1120.

19. Huet S, Tesson B, Jais JP, et al. A gene-expression profiling score for prediction of outcome in patients with follicular lymphoma: a retrospective training and validation analysis in three international cohorts. Lancet Oncol. 2018;19(4):549-561.

20. Silva A, Bassim S, Sarkozy C, et al. Convergence of risk prediction models in follicular lymphoma. Haematologica. 2019;104(6):e252-e255.

21. Rai S, Inoue H, Hanamoto H, et al. Low absolute lymphocyte count is a poor prognostic factor for untreated advanced follicular lymphoma treated with rituximab plus bendamustine: results of the prospective phase 2 CONVERT trial. Int J Hematol. 2021.

22. Cheson BD, Horning SJ, Coiffier B, et al. Report of an international workshop to standardize response criteria for non-Hodgkin's lymphomas. NCI Sponsored International Working Group. J Clin Oncol. 1999;17(4):1244.

23. Sakai K, Tsuboi M, Kenmotsu H, et al. Tumor mutation burden as a biomarker for lung cancer patients treated with pemetrexed and cisplatin (the JIPANG-TR). Cancer Sci. 2021;112(1):388-396.

24. Watatani Y, Sato Y, Miyoshi H, et al. Molecular heterogeneity in peripheral T-cell lymphoma, not otherwise specified revealed by comprehensive genetic profiling. Leukemia. 2019;33(12):2867-2883.

25. Rai S, Tanaka H, Suzuki M, et al. Chlorpromazine eliminates acute myeloid leukemia cells by perturbing subcellular localization of FLT3-ITD and KIT-D816V. Nat Commun. 2020;11(1):4147.

26. Sugio T, Miyawaki K, Kato K, et al. Microenvironmental immune cell signatures dictate clinical outcomes for PTCL-NOS. Blood Adv. 2018;2(17):2242-2252.

27. Huet S, Sujobert P, Salles G. From genetics to the clinic: a translational perspective on follicular lymphoma. Nat Rev Cancer. 2018;18(4):224-239.

28. Morin RD, Mendez-Lago M, Mungall AJ, et al. Frequent mutation of histone-modifying genes in non-Hodgkin lymphoma. Nature. 2011;476(7360):298-303.

29. Bouska A, Zhang W, Gong Q, et al. Combined copy number and mutation analysis identifies oncogenic pathways associated with transformation of follicular lymphoma. Leukemia. 2017;31(1):83-91.

30. Okosun J, Bödör C, Wang J, et al. Integrated genomic analysis identifies recurrent mutations and evolution patterns driving the initiation and progression of follicular lymphoma. Nat Genet. 2014;46(2):176-181.

31. Andor N, Simonds EF, Czerwinski DK, et al. Single-cell RNA-Seq of follicular lymphoma reveals malignant B-cell types and coexpression of T-cell immune checkpoints. Blood. 2019;133(10):1119-1129.

32. Béguelin W, Teater M, Meydan C, et al. Mutant EZH2 Induces a Pre-malignant Lymphoma Niche by Reprogramming the Immune Response. Cancer Cell. 2020;37(5):655-673.e611.

33. Boice M, Salloum D, Mourcin F, et al. Loss of the HVEM Tumor Suppressor in Lymphoma and Restoration by Modified CAR-T Cells. Cell. 2016;167(2):405-418.e413.

34. Devan J, Janikova A, Mraz M. New concepts in follicular lymphoma biology: From BCL2 to epigenetic regulators and non-coding RNAs. Semin Oncol. 2018;45(5-6):291-302.

35. Jurinovic V, Passerini V, Oestergaard MZ, et al. (2019) Evaluation of the m7-FLIPI in Patients with Follicular Lymphoma Treated within the Gallium Trial: EZH2 mutation Status May be a Predictive Marker for Differential Efficacy of Chemotherapy. Blood. 134: 122.

36. Bolen CR, Hiddemann W, Marcus R, et al: Treatment-dependence of high-risk gene expression signatures in de novo folicular lymphoma. International Conference on Malignant Lymphoma (ICML), June 18th-22nd, 2019, Abstract 143.

37. Inoue H, Rai S, Tanaka H, et al. Tumour-immune microenvironment in duodenal-type follicular lymphoma. Br J Haematol. 2020.

38. Voskoboinik I, Whisstock JC, Trapani JA. Perforin and granzymes: function, dysfunction and human pathology. Nat Rev Immunol. 2015;15(6):388-400.

39. Wu X, Wang X, Zhao Y, Li K, Yu B, Zhang J. Granzyme family acts as a predict biomarker in cutaneous melanoma and indicates more benefit from anti-PD-1 immunotherapy. Int J Med Sci. 2021;18(7):1657-1669.

40. de Vos S, Hofmann WK, Grogan TM, et al. Gene expression profile of serial samples of transformed B-cell lymphomas. Lab Invest. 2003;83(2):271-285.

41. Morschhauser F, Fowler NH, Feugier P, et al. Rituximab plus Lenalidomide in Advanced Untreated Follicular Lymphoma. N Engl J Med. 2018;379(10):934-947.

42. Leonard JP, Trneny M, Izutsu K, et al. AUGMENT: A Phase III Study of Lenalidomide Plus Rituximab Versus Placebo Plus Rituximab in Relapsed or Refractory Indolent Lymphoma. J Clin Oncol. 2019;37(14):1188-1199.

Tables

Due to technical limitations, table 1 and 2 is only available as a download in the Supplemental Files section.

Figures

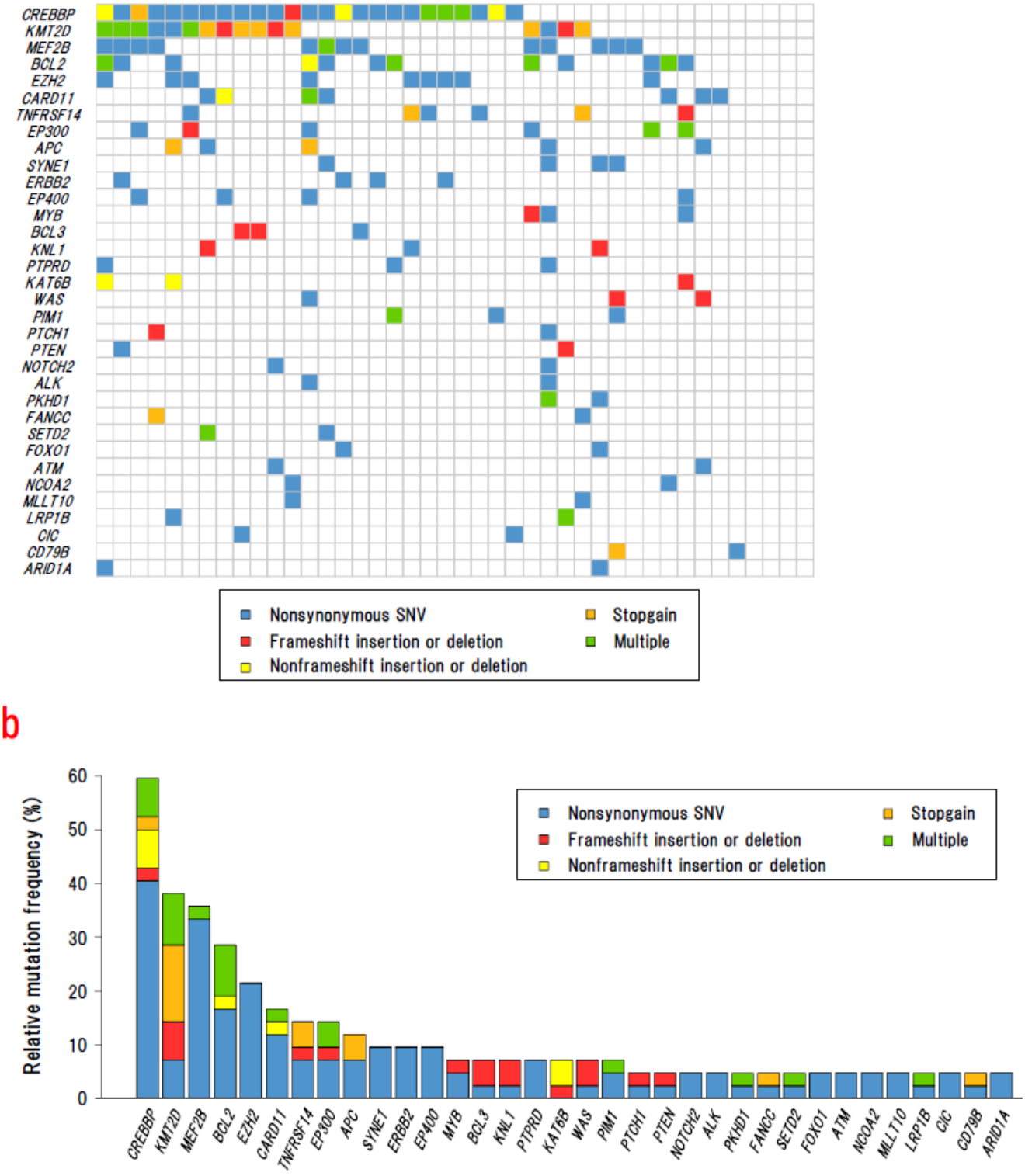

Figure 1

Landscape of somatic mutations. (a) Co-mutation plot showing the spectrum of recurrently mutated genes across all cases (n=42). (b) Frequencies and types of somatic mutations in 34 recurrently mutated genes (found in ≥2 cases) for all cases (n=42).

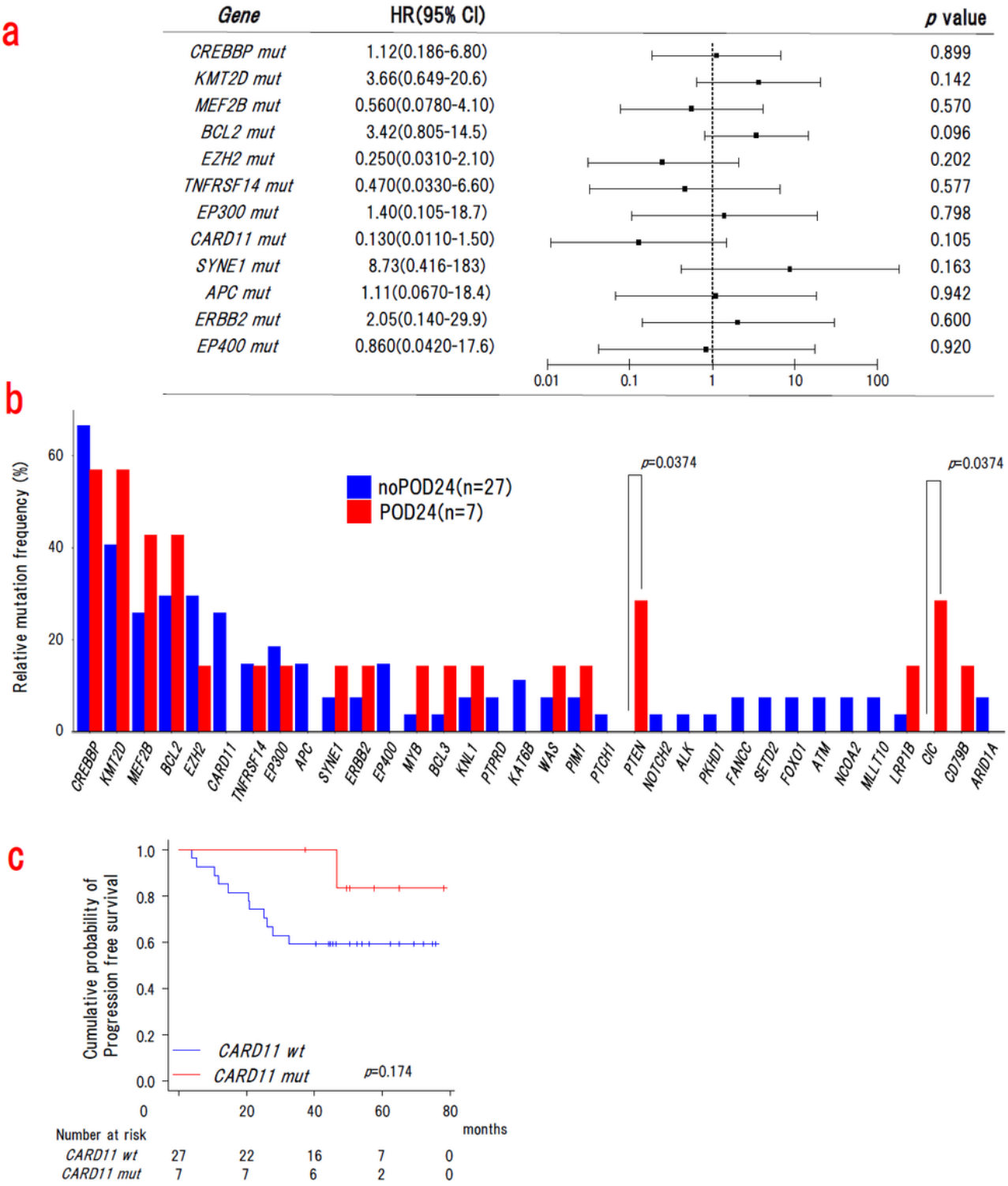

Figure 2

Association of mutation profile with clinical outcomes in the nOR-group (a) Forest plot for progression-free survival in univariate analyses. HR, hazard ratio. Mut, mutations. (b) Frequencies of mutations in 34 recurrently mutated genes in cases with or without POD24 in the nOR-group (n=34). p-values by Fisher's exact test were shown in the graphs. (c) Kaplan-Meier curves for progression-free survival of cases with

or without CARD11 mutations in the nOR-group (n=34). Log-rank p-values were shown in the graphs. Wt, wild type. Mut, mutations.

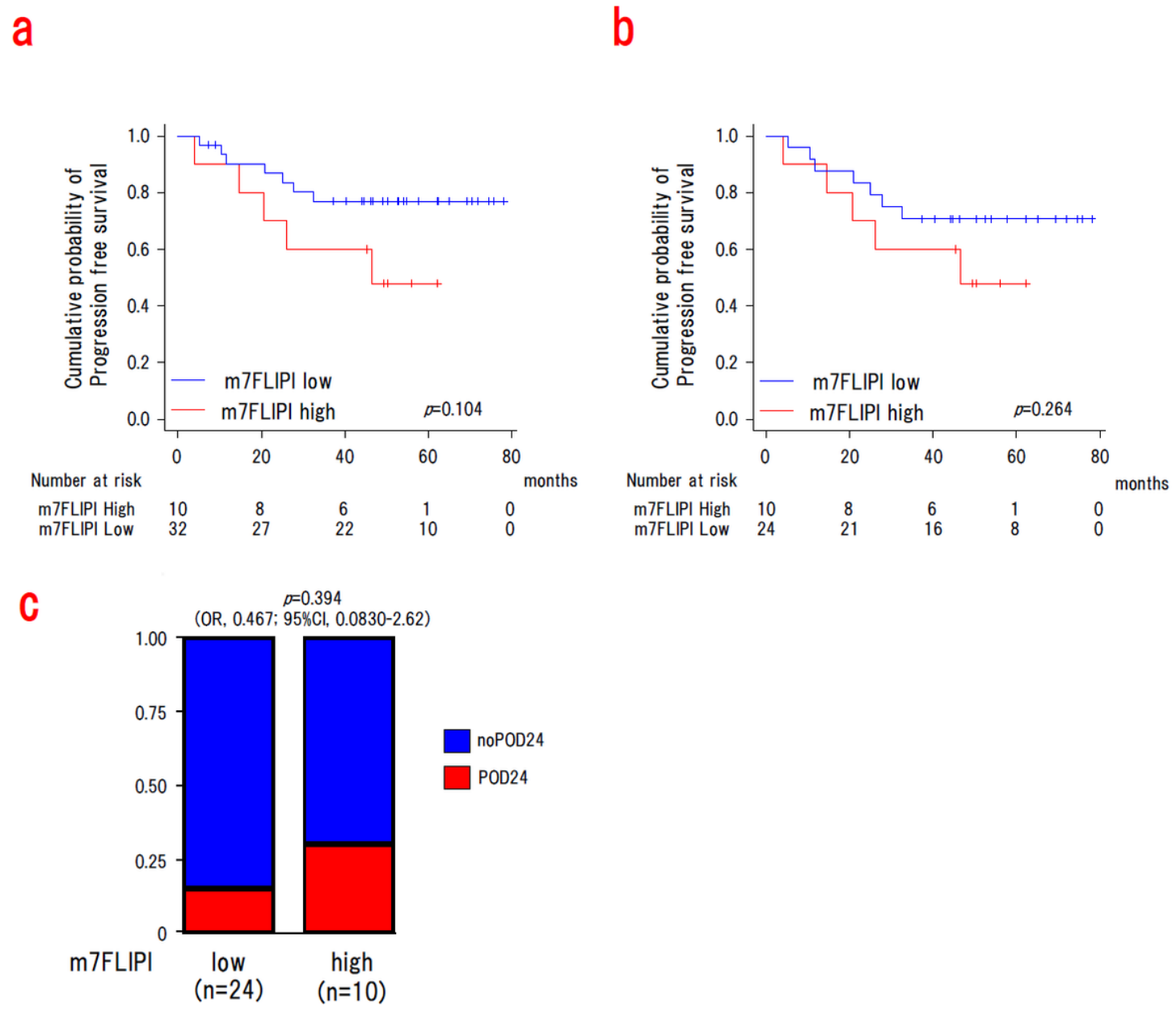

Figure 3

Association of m7-FLIPI with clinical outcomes Comparison of progression-free survival between the cases in the low- and high-risk categories classified by m7-FLIPI for (a) all patients (n=42) and (b) nOR-group (n=34). Log-rank p-values were shown in the graphs. Int, intermediate. (c) The proportions of the low and high-risk categories classified by m7-FLIPI in the cases with and without POD24 in the nOR-group (n=34). p-values by Fisher's exact test were shown in the graphs.

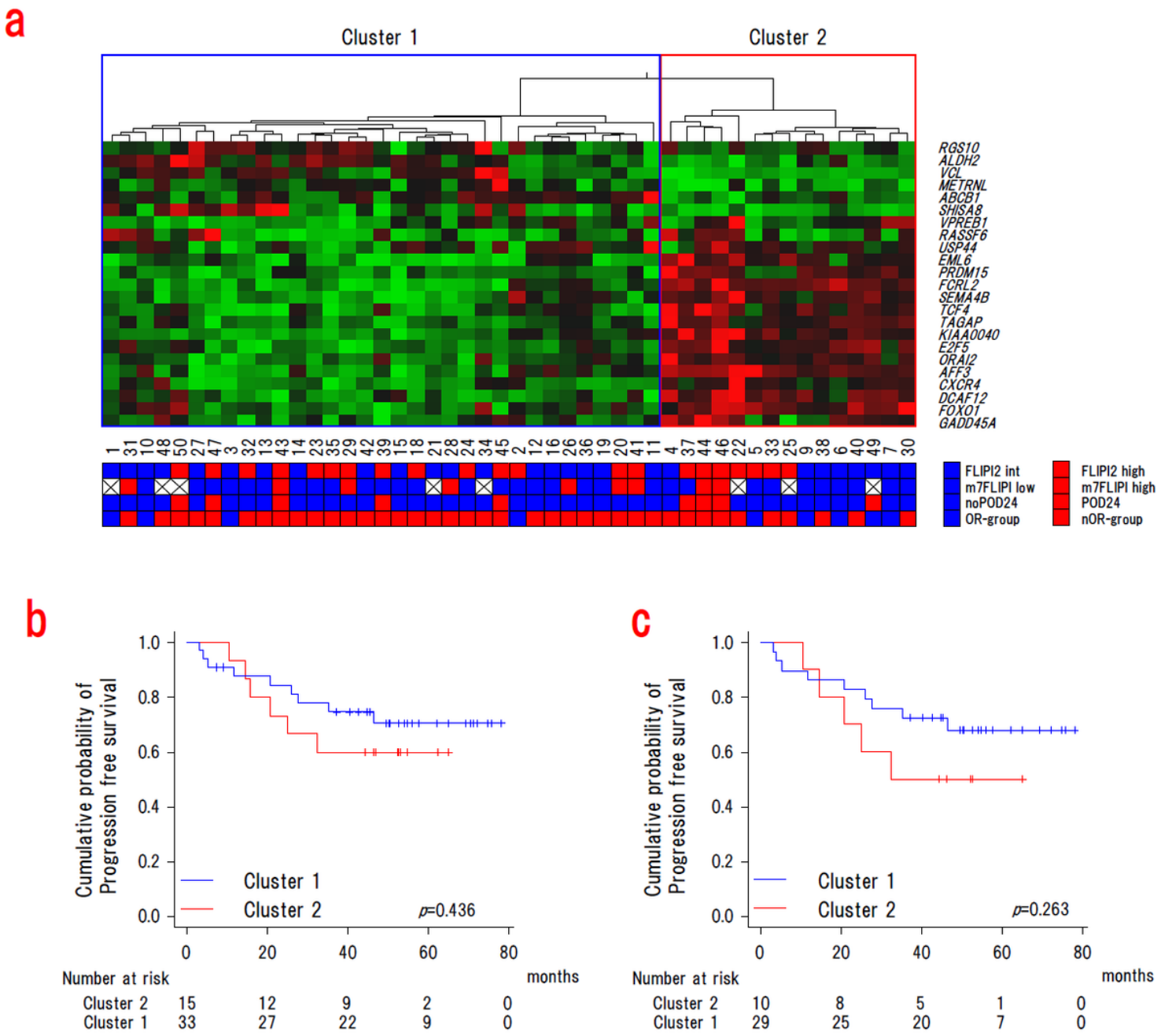

Figure 4

Association of the 23-gene expressions with clinical outcomes (a) Heat map and unsupervised, hierarchical clustering showing the genes along rows and cases along columns in all cases. Green denotes low and red indicates high gene expression. Cluster 1 and 2 were characterized by high expression of genes associated with favorable and poor outcome, respectively. (b) Kaplan-Meier curves for progression-free survival of cases with the cluster1 and 2 in all cases (n=48), (c) the nOR-group (n=39). Log-rank p-values were shown in the graphs.

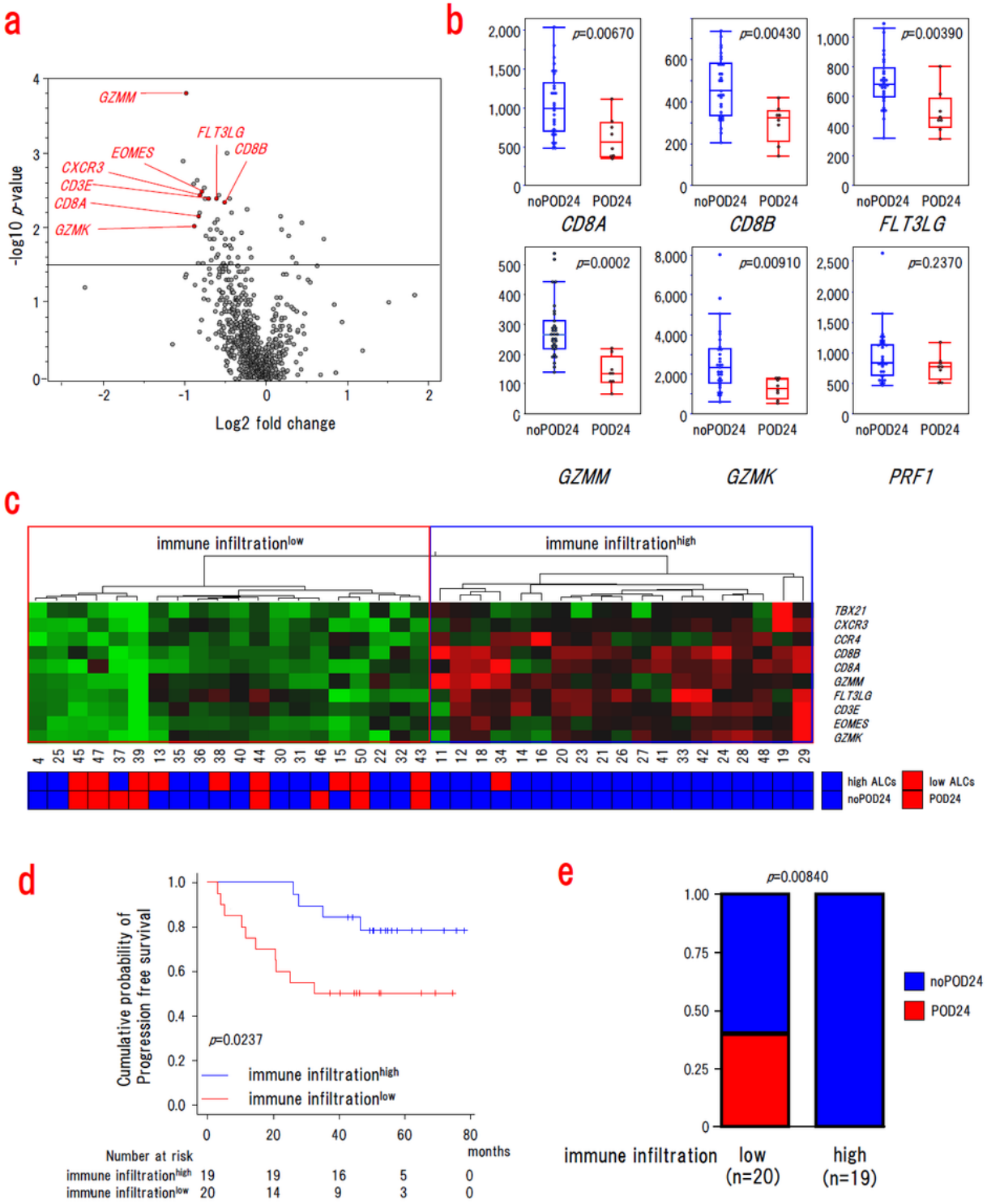

Figure 5

Association of the T-cell-associated genes expression with clinical outcomes (a) Volcano plot indicating differentially expressed genes in cases with and without POD24 in the nOR-group (n=39). (b) The gene expression levels of the CD8+ T-cell markers in the patients with POD24 and without POD24. p-values by Fisher's exact test were shown in the graphs. In box plots, the center line and lower and upper hinges correspond to the median, and the first and third quartiles (25 and 75 percentiles), respectively. The upper

and lower whiskers extend from the upper and lower hinges to the largest or smallest values no further than 1.5× inter-quartile range from the hinges. (c) Heat map and unsupervised hierarchical clustering showing the genes along rows and cases along columns in the nOR-group. Green denotes low and red indicates high gene expression. The regions indicated the low (shown in red) and high immune infiltration cluster (shown in blue), respectively. (d) Progression-free survival of cases in the low and high immune infiltration (infillow and infilhigh) clusters in the nOR-group (n=39). Log-rank p-values were shown in the graphs. (e) The proportion of cases with POD24 in the infillow and infilhigh clusters in the nOR-group. p-values by Fisher's exact test were shown in the graphs (n=39).

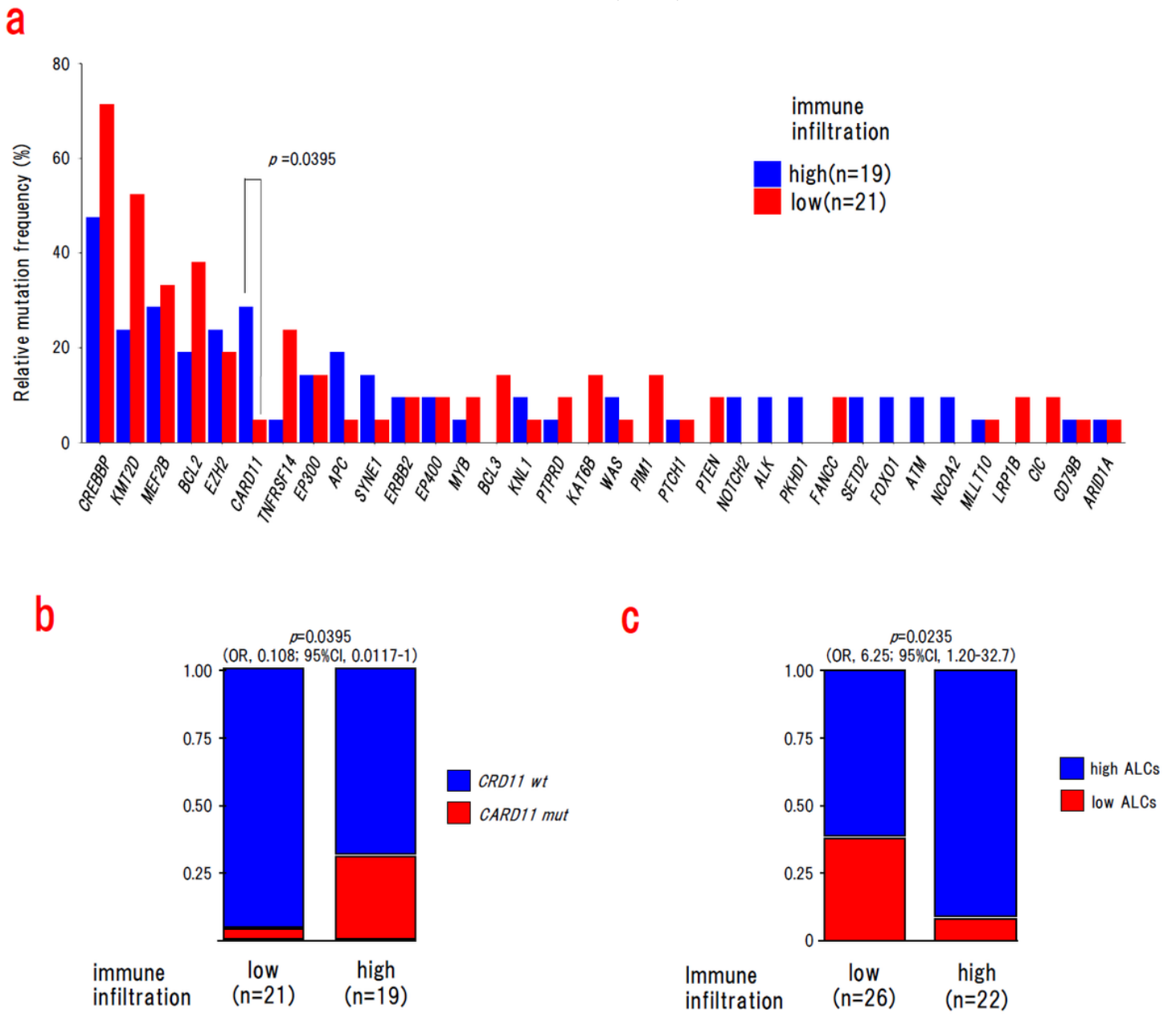

Figure 6

Association of the T-cell-associated genes expression with their mutation profile (a) Mutation frequencies of recurrently mutated genes by infillow and infilhigh clusters in all cases (n=40). p-values by Fisher's

exact test were shown in the graphs. (b) The proportion of cases with CARD11 mutations in the infillow and infilhigh clusters (n=40). p-values by Fisher's exact test were shown in the graphs. Wt, wild type. Mut, mutations. (c)The proportion of cases with low absolute lymphocyte counts in the infillow and infilhigh clusters (n=48). p-values by Fisher's exact test were shown in the graphs.

Supplementary Files

This is a list of supplementary files associated with this preprint. Click to download.

- Table1.xlsx
- Table2.xlsx
- Sourcedatafile1.xlsx
- Sourcedatafile2.xlsx
- SupplementaryMaterials.docx